



Performance of a magnesium–lithium alloy as an anode for magnesium batteries

A. SIVASHANMUGAM, T. PREM KUMAR, N.G. RENGANATHAN and S. GOPUKUMAR*

Central Electrochemical Research Institute, Karaikudi 630 006, INDIA

(*author for correspondence, e-mail: deepika_41@rediffmail.com)

Received 14 April 2004; accepted in revised form 14 June 2004

Key words: battery anode, magnesium–lithium alloy, polarization study, reserve battery

Abstract

In this work, we describe an evaluation of an Mg–Li alloy (Li: 13 wt %) for possible use in magnesium primary reserve batteries. Higher OCP for the Mg–Li alloy have been observed in 2 M MgCl_2 and MgBr_2 electrolyte. The corrosion rate of the Mg–Li alloy is found to be in the order: $\text{MgCl}_2 < \text{Mg}(\text{COOCH}_3)_2 < \text{MgSO}_4 < \text{MgBr}_2 < \text{Mg}(\text{ClO}_4)_2$. Mg–Li alloys exhibit higher (81%) anodic efficiencies even when the current density is increased to 8.6 mA cm^{-2} . It has been observed that Mg–Li/ MgCl_2 /CuO cells offer higher operating voltage and capacity than those with the conventionally used Mg–Al alloy.

1. Introduction

Magnesium batteries, both reserve and dry types, are attractive as power sources [1, 2]. Investigations on magnesium anodes individually or in conjunction with several depolarizers have been described [3–5]. The factors that favour the prospects of magnesium as an anode are high energy density, environmental-friendliness and technological viability [6].

Studies on the improvement of shelf-life and the potential of magnesium have been attempted through various means, for instance, by introducing inhibitors, eliminating certain impurity elements in the alloys, surface coating, and alloying with metals like Al, Zn, Pb, Sn, etc. Some magnesium alloys (AZ31, AZ21, AP65, AT61) have been investigated and a few are well established in practical applications [1, 7].

However, the idea of alloying lithium with magnesium is interesting. The aim is primarily to realize energy characteristics approaching that of lithium. However, very few reports [8–11] are available on the possibility of exploiting magnesium–lithium alloys as battery anodes. The addition of lithium to magnesium imparts corrosion resistance [12] similar to other magnesium alloys, while providing higher voltage and better discharge characteristics. Further, addition of lithium above 10% causes its crystal structure to become cubic and renders the alloy more ductile.

Hence, in the present study we have carried out a comprehensive investigation on the corrosion behaviour of Mg–Li (Li: 13 wt %) and Mg AZ31 alloys as well as on the performance characteristics of Mg–Li//CuO and Mg AZ31//CuO cells in selected electrolytes.

2. Experimental

2.1. Determination of self corrosion

The corrosion behaviour of magnesium depends on the concentration and pH of the electrolyte, composition of the alloy and on the nature of the constituents of the alloy. The corrosion behaviour has been studied using the weight loss method and galvanostatic polarization measurements.

2.1.1. Weight loss measurement

The weight loss is expressed in milligrams per square centimeter per minute. The self-corrosion of magnesium–lithium alloys in aqueous solutions of MgCl_2 , MgBr_2 , $\text{Mg}(\text{ClO}_4)_2$, MgSO_4 and $\text{Mg}(\text{COOCH}_3)_2$ at different concentrations were compared. Specimens of $1.0 \text{ cm} \times 1.5 \text{ cm}$ size were cleaned and dried. These sheets were completely immersed in 100 ml of the chosen electrolyte for 15 h at $30 \pm 1^\circ\text{C}$. These experiments were performed in unstirred solutions, mimicking actual battery conditions.

2.1.2. Galvanostatic polarization measurements

Anodic and cathodic polarization of the magnesium–lithium alloy was carried out by impressing a direct current from a constant current generator adopting the method of Wagner and Traud [13]. The experimental cell was a typical three-electrode assembly using platinum foil as counter, Ag/AgCl as reference and Mg–Li ($3 \text{ cm} \times 2 \text{ cm}$) as working electrodes. The Mg–Li pieces were cloth-buffed in the presence of pumice and then degreased with trichloroethylene. Polarization

measurements were started after an immersion time of 5 min when a steady-state potential (open-circuit potential) was attained. Current densities in the range of $10\text{--}250\text{ mA cm}^{-2}$ were impressed on the working electrode and the steady potential was measured at each current density. Current and potential measurements were made using a high-impedance multimeter.

2.2. Preparation of electrode and cell assembly

Mg–Li alloy sheets (containing 13 wt % of Li) of $3\text{ cm} \times 2\text{ cm}$ size and 0.15 cm thickness were used as the anode. Cathodes were prepared by pressing a loose powder mix containing 1 g of CuO, 0.4 g of acetylene black and 2–3 ml of an aqueous binder spread on both sides of a $3\text{ cm} \times 2\text{ cm}$ size copper mesh current collector of 20 mesh size under optimized pressure. The cathode plates were wrapped in cellophane sheets, which served as the separator. The number of cellophane layers varied between 2 and 4, depending on the rate of discharge of the cell. Thus, a cell assembly consisted of two anodes and a cathode separated by cellophane arranged alternately and loosely bound by a nylon thread for keeping the electrodes in place. The inter-electrode distance was carefully maintained such that it was small enough to keep the ohmic resistance low and large enough to allow for volume expansion of the anodes. The electrodes were assembled in a PVC container and activated with the required volume of electrolyte and discharged at constant current drains of 25, 50, 75 and 100 mA at room temperature up to a cut-off voltage of 0.8 V. Voltage vs time was recorded at regular time intervals. The weight of anode consumed was also determined from the weights of the anodes taken before and after discharge. At the end of each experiment, the anodes were removed and subsequently cleaned in the cleaning solution before weighing.

3. Results and discussion

The work described here relates to the study of the anodic behaviour of Mg–Li alloy undertaken either individually or in combination with cathode in the presence of electrolytes such as MgCl_2 , MgBr_2 , $\text{Mg}(\text{ClO}_4)_2$, MgSO_4 and $\text{Mg}(\text{COOCH}_3)_2$.

3.1. Corrosion rate measurements

It is well known that the corrosion rate depends on electrolyte concentration, alloy composition, and solution pH. For example, the corrosion rate of Mg–Al alloys is the highest in chloride medium and lowest in perchlorate medium. This was ascribed to parasitic corrosion occurring in Mg–Al alloys [14, 15].

However, in Mg–Li alloy, the rate of corrosion is maximum and minimum in $\text{Mg}(\text{ClO}_4)_2$ and MgCl_2 electrolyte solutions, respectively (Table 1). Further, the corrosion rate increased with increase in electrolyte

Table 1. Corrosion rates of Mg–Li alloy in different electrolytes

Electrolyte	Corrosion rate / $\text{mg cm}^{-2} \text{ min}^{-1}$		
	1.0 M	1.5 M	2.0 M
MgCl_2	0.0031	0.0042	0.0059
MgBr_2	0.0046	0.0057	0.0168
$\text{Mg}(\text{ClO}_4)_2$	0.0054	0.0074	0.0422
MgSO_4	0.0038	0.0052	0.0072
$\text{Mg}(\text{COOCH}_3)_2$	0.0053	0.0060	0.0067

concentration. The corrosion rates of Mg–Li alloy in 2 M solutions of the various electrolytes are in the order: $\text{MgCl}_2 < \text{MgSO}_4 < \text{Mg}(\text{COOCH}_3)_2 < \text{MgBr}_2 < \text{Mg}(\text{ClO}_4)_2$. Table 2 presents a comparison of the corrosion rate of Mg–Li alloy with the widely used Mg AZ31 alloy. The maximum and minimum rates of corrosion are observed with Mg–Li alloy in $\text{Mg}(\text{ClO}_4)_2$ and MgCl_2 electrolyte solutions, respectively. The above observations are interesting considering the difference in the corrosion behaviour of Mg–Al and Mg–Li alloys. In the case of Mg–Al alloys, the onset of parasitic reactions and subsequent formation of the highly acidic AlCl_3 salt enhance the rate of corrosion in MgCl_2 medium. However, in Mg–Li alloy, the anodically generated LiCl accumulates until it precipitates out as an impervious layer [16] in the pores of the superficial hydroxide layer and, thereby, increases the corrosion resistance of this alloy. Further, these facts may also be supplemented by mechanical properties associated with the alloy [8].

3.2. Open-circuit potential measurements

Open-circuit potential (OCP) measurements were carried out for Mg–Li alloy (vs Ag/AgCl) in 1.0, 1.5 and 2.0 molar concentrations of MgCl_2 , MgBr_2 , $\text{Mg}(\text{ClO}_4)_2$, MgSO_4 and $\text{Mg}(\text{COOCH}_3)_2$ electrolytes. These potentials represent the level of coverage of metal by a protective film – the greater the protection, the less the potential.

It is evident from Table 3 that the OCP of Mg–Li alloy increases slightly with increasing electrolyte concentration. The OCP is marginally higher in the case of MgCl_2 or MgBr_2 electrolyte, and this may be ascribed to the slightly acidic nature [4] of these electrolytes. It is

Table 2. Corrosion rates of Mg–Li and Mg AZ31 alloy in 2.0 M electrolytes

Electrolyte	Corrosion rate / $\text{mg cm}^{-2} \text{ min}^{-1}$	
	Mg–Li	Mg AZ31
MgCl_2	0.0059	0.1832
MgBr_2	0.0168	0.0810
$\text{Mg}(\text{ClO}_4)_2$	0.0422	0.0029
MgSO_4	0.0072	0.0033
$\text{Mg}(\text{COOCH}_3)_2$	0.0067	0.0034

Table 3. Open-circuit potentials of Mg–Li alloy in various electrolytes with respect to Ag/AgCl reference electrode

Electrolyte	Open-circuit potential /V		
	1.0 M	1.5 M	2.0 M
MgCl ₂	–1.46	–1.48	–1.50
MgBr ₂	–1.47	–1.48	–1.52
Mg(ClO ₄) ₂	–1.42	–1.42	–1.44
MgSO ₄	–1.36	–1.39	–1.42
Mg(COOCH ₃) ₂	–1.38	–1.40	–1.46

interesting to compare our observations with the OCP of Mg–Al alloys [14], for which higher potential differences are realized in MgCl₂ medium than in Mg(ClO₄)₂ which is as much as 0.15 V. However, in the present study the difference is only 0.06 V. This fact may be ascribed to an adherent passive film formed by LiCl. The formation of corrosion products arising from the high reactivity of the alloy, the consequent rise in the internal resistance and the partial coverage of the electrode surface by hydrogen, which leads to a reduction in the effective surface area, are among reasons for the sharp drop in OCP of these alloys.

3.3. Galvanostatic polarization measurements

Figures 1–3 show plots of potential against log current density for Mg–Li alloy in various electrolytes when subjected to galvanostatic polarization. It is observed that the cathodic polarization region was more pronounced than the anodic polarization region. This reveals that the corrosion of these alloys is controlled

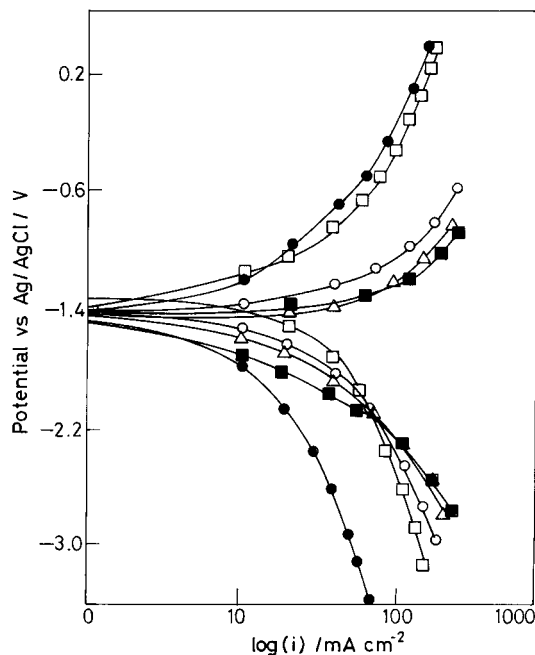


Fig. 1. Galvanostatic polarization curves of Mg–Li alloy in various electrolytes at 1 M concentration. Δ – MgCl₂, \square – MgSO₄, \blacksquare – MgBr₂, \bullet – Mg(COOCH₃)₂, \circ – Mg(ClO₄)₂.

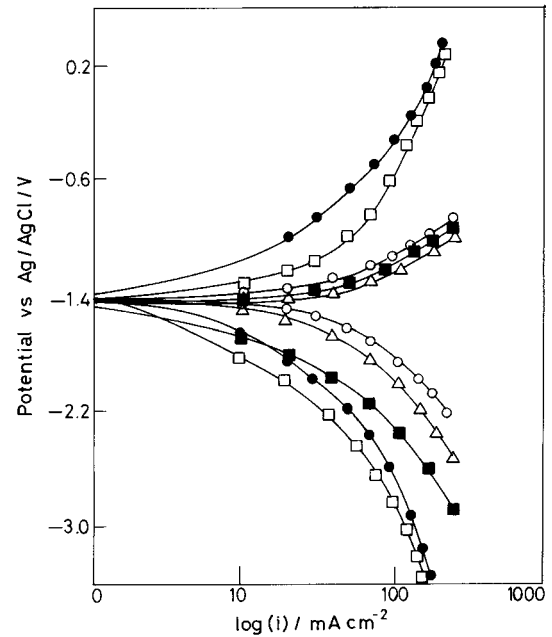


Fig. 2. Galvanostatic polarization curves of Mg–Li alloy in various electrolytes at 1.5 M concentration. Δ – MgCl₂, \square – MgSO₄, \blacksquare – MgBr₂, \bullet – Mg(COOCH₃)₂, \circ – Mg(ClO₄)₂.

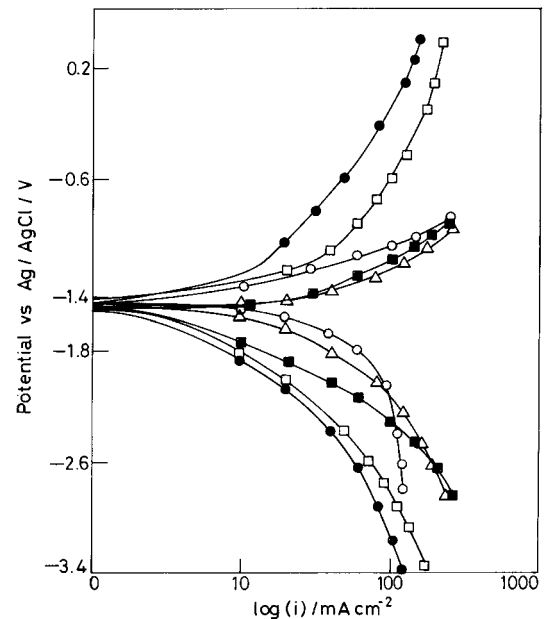


Fig. 3. Galvanostatic polarization curves of Mg–Li alloy in various electrolytes at 2 M concentration. Δ – MgCl₂, \square – MgSO₄, \blacksquare – MgBr₂, \bullet – Mg(COOCH₃)₂, \circ – Mg(ClO₄)₂.

cathodically. A similar behaviour is observed in the case of Mg AZ31 alloy (Figures 4–6). It can be seen that MgSO₄ and Mg(COOCH₃)₂ show more positive value and hence these electrolytes are not suitable.

3.4. Discharge behaviour

Magnesium reserve cells were fabricated using Mg–Li alloy as anode and CuO as cathode. The discharge characteristics of Mg–Li/MgCl₂/CuO cells were

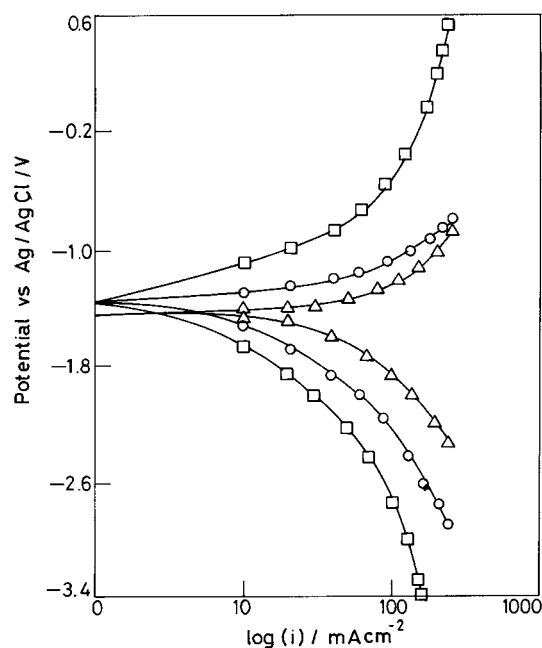


Fig. 4. Galvanostatic polarization curves of Mg AZ31 alloy in various electrolytes at 1 M concentration. Δ – MgCl_2 , \circ – $\text{Mg}(\text{ClO}_4)_2$, \square – MgSO_4 .

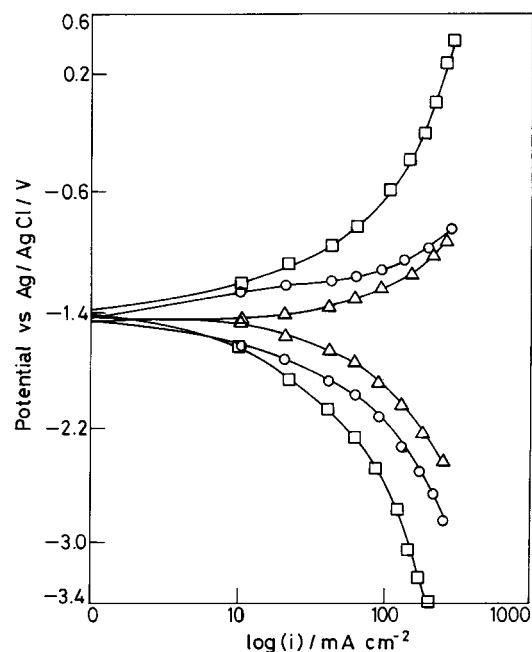


Fig. 6. Galvanostatic polarization curves of Mg AZ31 alloy in various electrolytes at 2 M concentration. Δ – MgCl_2 , \circ – $\text{Mg}(\text{ClO}_4)_2$, \square – MgSO_4 .

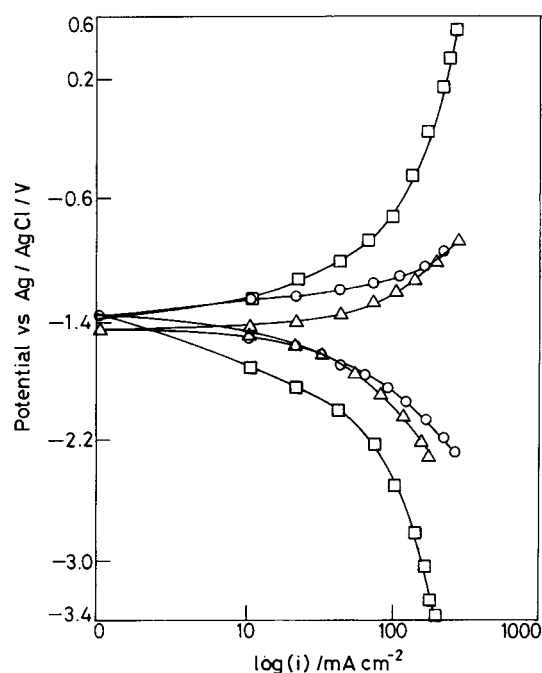


Fig. 5. Galvanostatic polarization curves of Mg AZ31 alloy in various electrolytes at 1.5 M concentration. Δ – MgCl_2 , \circ – $\text{Mg}(\text{ClO}_4)_2$, \square – MgSO_4 .

recorded under continuous galvanostatic discharge at various current densities. Table 4 summarizes the performance of the above cell at various current drains (25, 50, 75 and 100 mA) corresponding to current densities of 2.1, 4.2, 6.3, 8.3 mA cm^{-2} , respectively. An increase in the current density results in a loss of cell capacity, which may be attributed to increased cathodic polarization during discharge.

Table 4. Various energy parameters of Mg–Li/MgCl₂/CuO cells

Cell parameters	Current density / mA cm^{-2}			
	2.1	4.2	6.3	8.6
Cell voltage (V)	1.24	1.06	0.92	0.87
Capacity (Ah)	0.64	0.63	0.40	0.35
No. of electrons transferred	1.91	1.86	1.19	1.04
Cathodic efficiency (%)	95	93	60	53
Anodic efficiency (%)	65	68	73	81

Figure 7 shows the discharge behaviour of Mg–Li/MgCl₂/CuO cells. The open-circuit voltage of 1.62 V decreased on applying a load to a constant working voltage of 1.24 V. This also reflects the internal resistance of the cell. The capacity output, or the cathode efficiencies, were 95% and 53% at the lower and higher current drains, respectively, indicating higher electron transfer efficiency at the lower drains. A comparison of these results with those obtained with the Mg AZ31/CuO cell at 25 and 50 mA current drains (Figure 7) suggests that the incorporation of lithium not only increases the operating voltage by 0.3–0.4 V but also enhances the cell capacity. This may be explained as due to the cubic crystal structure of this alloy [12]. These results are in agreement with earlier assumptions [17].

The anodic efficiencies of Mg–Li/MgCl₂/CuO cells at various current densities are presented in Table 4. It is seen that the efficiencies increase with increasing current densities. For example, at a current density of 8.6 mA cm^{-2} , the efficiency was 81%. This may be due to the high concentration of hydroxyl ions which can

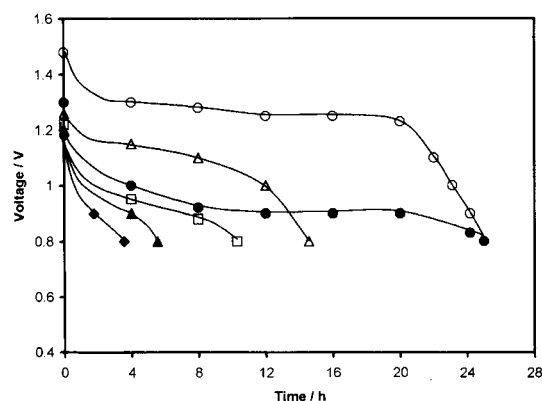


Fig. 7. Discharge behaviour of Mg-Li/CuO and Mg AZ31/CuO cells at various current drains. Mg-Li Cell: \circ – 25 mA; \triangle – 50 mA; \blacktriangle – 75 mA; \blacklozenge – 100 mA. Mg AZ31 Cell: \bullet – 25 mA; \square – 50 mA.

generate thick $\text{Mg}(\text{OH})_2$ films as well as passivation of lithium caused by the MgCl_2 in superficial anolytes. The above facts are in agreement with the observations of Wiesener et al. [18].

4. Conclusions

Corrosion behaviour of a magnesium–lithium alloy (Li: 13 wt %) was studied by means of polarization studies and weight loss measurements in various magnesium salt electrolytes. The suitability of the alloy as an anode for battery application was investigated and the following conclusions were arrived at.

1. Mg–Li alloy exhibits high OCP values in MgCl_2 and MgBr_2 electrolytes.
2. The corrosion rate of Mg–Li alloy is found to be in the order: $\text{MgCl}_2 < \text{Mg}(\text{COOCH}_3)_2 < \text{MgSO}_4 < \text{MgBr}_2 < \text{Mg}(\text{ClO}_4)_2$.
3. Mg–Li alloy exhibits higher anodic efficiencies (81%) even when the current density is increased to 8.6 mA cm^{-2} .

4. Mg–Li/ MgCl_2 /CuO cells give higher operating voltages and capacities than similar cells employing Mg–Al alloy as anode.
5. Galvanostatic polarization studies demonstrate that the corrosion of Mg–Li in MgCl_2 , MgBr_2 , $\text{Mg}(\text{ClO}_4)_2$, MgSO_4 and $\text{Mg}(\text{COOCH}_3)_2$ electrolytes is cathodically controlled.
6. In view of the above advantages, Mg–Li alloy (containing 13 wt % of Li) is a potential anode material for magnesium batteries.

References

1. G.W. Heise and C.N. Cahoon, 'Primary Batteries', Vol. 1 (John Wiley & Sons, Inc. N.Y., USA, 1960).
2. L. Jarvis, *J. Power Sources* **32** (1990) 271.
3. Gopukumar, A. Sivashanmugam and N. Muniyandi, *J. Power Sources* **38** (1992) 121.
4. Gopukumar, A. Sivashanmugam and N. Muniyandi, *J. Appl. Electrochem.* **23** (1993) 265.
5. Gopukumar, A. Sivashanmugam and R. Sridharan, *J. Electrochem. Soc.* **140** (1993) 3087.
6. T.D. Gregory, R.J. Hoffman and R.C. Winterton, *J. Electrochem. Soc.* **137** (1990) 775.
7. N.C. Cahoon and G.V. Heise, 'Primary Batteries', Vol. 2 (John Wiley & Sons, Inc. N.Y., USA, 1976).
8. Y. Iwadata, M. Lassouani, F. Lautelme and M. Chemia, *J. Appl. Electrochem.* **17** (1987) 385.
9. M.L. Saboungi and M. Blander, *J. Electrochem. Soc.* **122** (1975) 1631.
10. V.S. Tiunov, A.G. Morachevskii and A.I. Demidov, *J. Appl. Chem. (USSR)* **52** (1979) 2454.
11. E.N. Protasov, A.A. Gnilomedov and A. L. L'vov, *Sov. Electrochem.* **14** (1978) 1127.
12. M. Sahoo and J.T.N. Atkinson, *J. Mater. Sci.* **17** (1982) 3564.
13. C. Wagner and W. Traud, *Z. Phys. chem.* (1938) 411.
14. R. Udhayan, N. Muniyandi and P.B. Mathur, *Brit. Corr. J.* **27** (1992) 68.
15. R. Udhayan and D.P. Bhatt, *J. Power Sources* **39** (1992) 107.
16. S.D. James, in *Proc. Symposium on Lithium Batteries* (1984) p. 18.
17. R. Jasinsky, 'High Energy Batteries' (Plenum Press, N.Y., USA, 1967).
18. L. Wiesener, W. Glaeser and R. Peiz, 'Power Sources 5' (Academic Press, London, 1975).